Strength of Steel Culvert Sheets Bearing Against Compacted Sand Backfill

G. G. MEYERHOF, Director, School of Graduate Studies, Nova Scotia Technical College, Halifax, and
L. D. BAIKIE, Engineer, Materials Testing Laboratory, Department of Public Works, Ottawa, Ontario

As part of a study of the strength of corrugated metal culverts under fills, an investigation has been made of the ultimate load of curved steel sheets bearing against dense sand backfill. The loading tests were carried out at a scale of one-eight full size by applying an axial load at the end of plain and corrugated sheets of various thicknesses and radii of curvature. During the tests measurements were made of the strains, soil pressures and deflections of the sheets.

The stress-deformation and strength characteristics of the sand were determined by triaxial compression tests from which representative values of the coefficient of soil reaction ("subgrade modulus") were calculated. These values were found to be of the same order as the average coefficients deduced from the loading tests on the sheets. Using these coefficients, the theoretical ultimate load of the sheets was determined from an analysis based on an extension of the theory of elastic stability of plates to the problem of curved sheets supported by an elastic medium.

The analysis shows that for small values of the coefficient of soil reaction or modulus of deformation of the soil, and for small values of the flexural rigidity of the plates, the sheets would fail by buckling, but for larger values of these parameters the sheets would fail by yielding of the section. The observed ultimate loads and modes of failure of the sheets were in reasonable agreement with these estimates and also support the ring compression theory.

An analysis is also made of the strength of flexible culverts under fills, for which simple equations and design charts are presented. From the results of field observations on the deformation of flexible culverts, minimum values of the coefficient of soil reaction and modulus of deformation of fills are suggested to insure that the critical stresses are sensibly independent of the culvert diameter. The results of some earlier model tests on the buckling of flexible culverts support the proposed method of analysis, which can be used in conjunction with the ring compression theory to estimate the strength of culverts under fills in practice.

• THE RAPID expansion of modern transportation facilities requires the construction of numerous culverts and other underground structures. Since many of these installations are of greater size and subjected to larger loads than those built previously,

Paper sponsored by Committee on Culverts and Culvert Pipe.

an estimate of the strength of such structures has to be based on an extension of previous experience through rational methods of design.

One of the best known analyses of the behavior of flexible circular culverts under an earth fill is that of Spangler (3) who extended Marston's theory of loads on underground pipes. In this method the vertical pressures are assumed to be uniformly distributed over the pipe diameter at the top and over the bedding width at the bottom of the culvert. The horizontal pressure is assumed to be distributed parabolically over the middle 100° arc of the pipe, and the resulting stresses and deflection of the pipe are evaluated. This approach has recently been simplified by White (8) who assumed a uniform pressure distribution around flexible pipes with sufficient cover and good backfill so that the strength of culverts can then be estimated from the simple theory of ring compression.

Both methods neglect instability of culverts due to buckling which was discussed by Watkins (6) on the assumption of a uniform pressure distribution around circular culverts. Since buckling may govern the strength of larger culverts and the pressure distribution around such structures is not necessarily uniform, an investigation was made at the Nova Scotia Technical College of the ultimate load of steel culvert sheets bearing against dense sand backfill. The loading tests were carried out at a scale of one-eighth full size, and measurements were made of the strains, soil pressures and deflections of the sheets (1). This report summarizes the main test results and extends previous analyses to an estimate of the ultimate strength of flexible culverts in practice.

METHOD AND RESULTS OF MODEL TESTS

Underground flexible culverts frequently have their critical sections in the lower quadrants due to difficulties of obtaining a uniform backfill. Quarter-sections of a circular culvert were therefore selected for the present tests, and for testing convenience and analysis, an axial load was applied directly to the end of the sheets (Fig. 1). This loading condition is more severe than that found in practice where the load is applied to culverts through an earth fill.

The model tests were carried out in a steel box about $4\frac{1}{2}$ ft long, 2 ft wide and 3 ft high (Fig. 1). The plain and corrugated steel sheets had about a 19-in. width and 12- and 24-in. nominal radii. The physical properties of the steel culvert sheets are given in Table 1. Electric resistance strain gages, soil pressure gages and dial deflectometers were mounted along the central arc of the sheets (Fig. 1). The soil pressure gages consisted of lead plates of $\frac{1}{2}$-in. diameter and $\frac{1}{16}$-in. thickness, which were indented by $\frac{1}{8}$-in. diameter steel balls attached to the sheets. Using a calibration curve based on the average duration of the tests, the maximum soil pressures could readily be deduced from the diameter of the indentation in the lead.

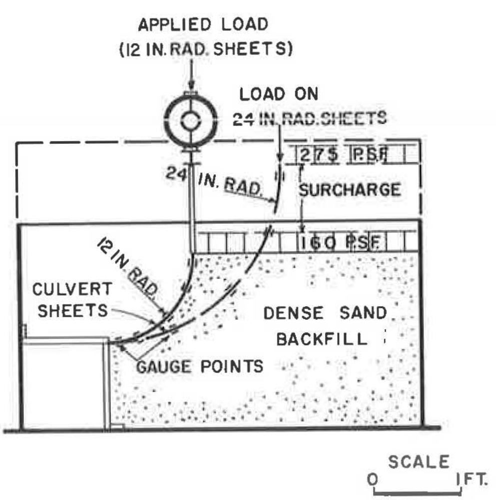

Figure 1. General arrangement of loading tests.

During the backfilling and compaction of the dry sand (Table 2), the sheets were supported by bracing. This was removed before a surcharge was placed on the sand, representing the weight of the soil above the centerline of the culvert plus a 3-ft cover at $\frac{1}{8}$ scale of the tests. The upper and lower edges of the sheets were free to rotate during the tests, and in some cases an attempt was made to prevent shear at the upper edge by allowing horizontal movement of the load.

The main test results are summarized in Table 3. It was found that both stresses and radial deflections of the sheets increased roughly linearly with the load until

TABLE 1

PROPERTIES OF STEEL CULVERT SHEETS

Sheet Type	Test No.	Radius, r (in.)	Thickness, t (in.)	Area, A (sq in.)	Yield Stress, f_y (psi)
Plain	1 and 2	12	0.042	0.788	45,000
	3 and 4	12.9	0.042	0.788	45,000
	5[a]	12.9	0.017	0.319	35,000
	6	25.6	0.042	0.788	45,000
	7[a], 8[a], and 9	12.9	0.017	0.319	35,000
Corrugated[b]	10	12	0.017	0.427	30,000
	11	24	0.017	0.386	30,000
	12	24	0.017	0.388	30,000
	13	12	0.017	0.396	30,000

[a]No shear test.
[b]Corrugations: 1/4 x 3/4 in.

TABLE 2

PROPERTIES OF SAND BACKFILL[a]

Effective size, d_{10}	0.16 mm
Uniformity coeff., U	5.0
Avg. unit weight, w	116 pcf
Relative density, D_r	0.9
Angle of intnl. frict., ϕ	40°

[a]Grading limits: No. 200 to 4 U.S.S.sieve.

failure was reached, except near the critical section where the increase was more rapid as the ultimate load was approached. At any given load, the observed axial stresses decreased with distance from the upper edge of the sheet (Fig. 2) on account of the skin friction between the sheets and the sand, and the deduced angle of skin friction of about 20° agrees well with previous investigations for smooth metal (2). Because of this skin friction and the limited lateral restraint near ground level, failure of the sheets occurred within the upper 2 in. in most tests. The average radial failure strain was generally of the order of $\frac{1}{4}$ to $\frac{1}{2}$ percent of the radius of the sheets; the corresponding vertical strain at the upper edge was about $\frac{1}{2}$ to 1 percent of the radius of the sheets.

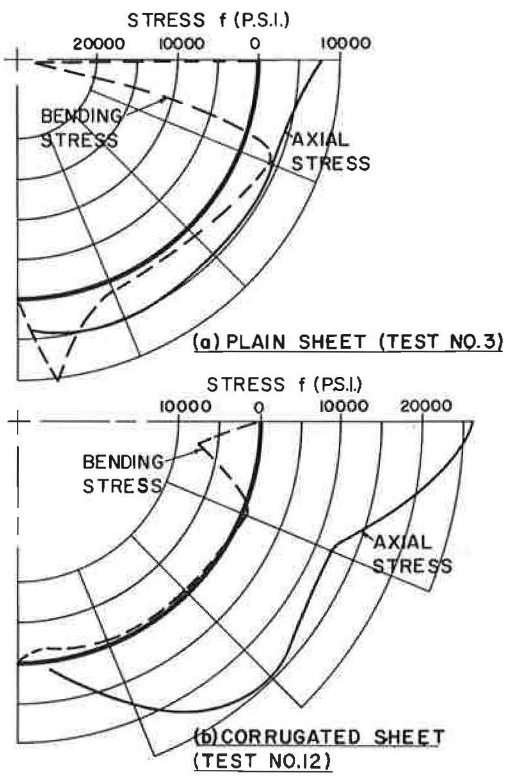

Figure 2. Stresses in sheets at ultimate load.

All plain sheets failed by buckling and, omitting the exceptionally low value of test No. 1 due to accidental eccentricity of the load, the average failure stress of the thin sheets was about 7,100 psi and for thick sheets about 5,600 psi. Both values represent about 16 percent of the corresponding yield stress of the material. The sheets without

TABLE 3

RESULTS OF LOADING TESTS ON CULVERT SHEETS

Test No.	Obs. Ult. Load, P_0 (lb)	Max. Axial Stress, f_0 (psi)	Avg. Soil Pressure, p (psi)	Avg. Radial Deflect., d (in.)	Avg. Coef. of Soil React., k (pci)	Theoret. Ring Stress, Eq. 1, f_a (psi)	Theoret. Critical Stress, Eq. 2, f_c (psi)
1	1,730[a]	2,190[a]	5.0	0.013	385	1,540	12,000
2	5,000	6,350	8.6	0.043	200	2,640	8,820
3	6,180	7,850	3.6	0.076	45	1,100	4,200
4	6,900	8,770	11.9	0.074	160	3,680	7,800
5	1,840	5,780	8.1	0.022	370	6,160	6,920
6	4,400	5,600	5.9	0.057	105	3,380	6,250
7	2,490	7,800	8.3	0.029	285	6,290	6,000
8	1,500	4,690	6.9	0.026	260	5,250	5,780
9	1,270	3,980	7.0	0.015	465	5,290	7,750
10	14,200	33,300	48.1	0.224	215	33,900	(97,000)
11	7,800	20,100	6.6	0.029	225	9,310	(100,000)
12	10,100	26,100	3.7	0.030	125	5,230	(73,000)
13	16,400	41,400	36.7	0.432	85	25,900	(60,000)

[a]Low value due to eccentric load.

shear at the upper edge carried somewhat larger loads than those with shear as would be expected. On the other hand, the corrugated sheets generally failed by crushing at an average stress of about 30,000 psi which is the same as the yield stress of the steel. Except near the critical section and lower edge, the bending stresses in the sheets were small and amounted to about ¼ to ½ the axial stresses at failure in the central portion of the sheets (Fig. 2).

Although the distribution of the soil pressure on the sheets at failure is similar to the maximum radial deflections, the observed coefficients of soil reaction (ratios of soil pressure to radial deflection) varied considerably around the sheets and increased as the radial deflection decreased (Fig. 3). Therefore, the average values of the soil pressure, radial deflection and coefficient of soil reaction (Table 3) were obtained by dividing the total volume under the pressure and deflection curves by the area of the sheets in contact with the sand.

ANALYSIS OF TEST RESULTS

If the flexural rigidity of the sheets is ignored, the average axial stress f_a in a cylindrical plate can be estimated from the theory of ring compression (8) so that

$$f_a = pr/A \tag{1}$$

in which

p = average soil pressure on plate;
r = radius of plate; and
A = cross-sectional area of plate.

Using the average observed soil pressures at failure and the original radius of the sheets, the calculated ring stresses are found to be of a similar order of magnitude as the observed maximum axial stresses (Table 3). The main differences between the estimates and observations are associated with low soil pressures for which the pressure gages were rather insensitive.

Another estimate of the failure stresses can be obtained from the theory of elastic stability of plates (5). If a cylindrical plate bearing against compact soil is compressed by a uniformly distributed force acting on the straight and hinged edges, the theoretical buckling stress is

$$f_b = \frac{2}{A}\sqrt{\frac{kEI}{1 - m^2}} \qquad (2)$$

in which

A = cross-sectional area of plate;
E = modulus of elasticity of plate;
I = moment of inertia of plate;
k = coefficient of soil reaction (subgrade modulus); and
m = Poisson's ratio of plate.

The maximum value of the buckling stress f_b is given by the yield stress f_y of the plate (see Appendix).

The average values of the coefficient of soil reaction k can be approximately determined from the modulus of deformation E_s of the soil in triaxial compression tests under a lateral pressure equal to the average confinement pressure of the soil (4), which was about 10 psi at the center of the sheets at failure. Making an 18-in. allowance behind the sheets for the limited width of backfill, the coefficients of soil reaction deduced from triaxial compression tests on the sand are shown in Figure 4 together with the average values obtained from the loading tests. While these coefficients are roughly inversely proportional to the radial deflection, the coefficients from the loading tests are somewhat larger than the values deduced from the triaxial compression tests because of the skin friction between the sand and both the sheets and the steel box. This makes the sand appear to be stiffer than assumed.

Using the coefficients of soil reaction from the loading tests, the critical stresses estimated from Eq. 2 are given in Table 3. The estimated critical stresses compare reasonably well with the observed maximum values and also support the observed mode of failure of the sheets. Thus, the estimates show that the plain sheets are expected to fail by buckling at a stress of the order of one-sixth of the yield stress of the steel, while the corrugated sheets are expected to fail by crushing at the

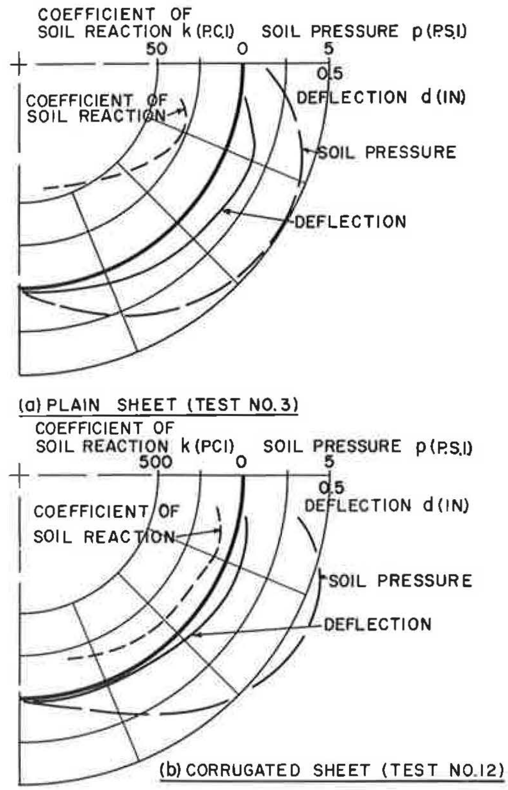

Figure 3. Soil pressures, deflections, and coefficients of soil reaction for sheets at ultimate load.

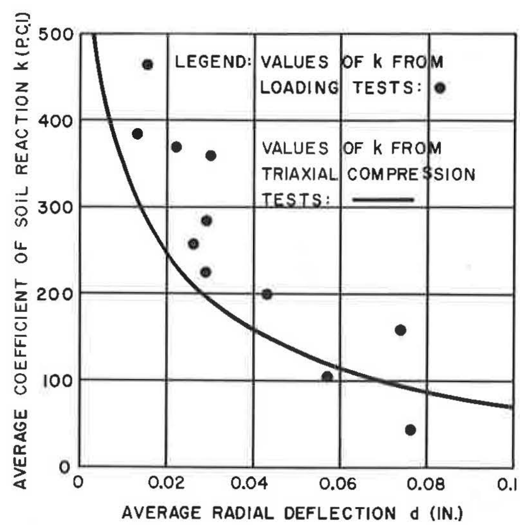

Figure 4. Coefficients of soil reaction from loading tests and triaxial compression tests.

yield stress since their theoretical buckling stress is some 2 to 4 times the yield stress.

STRENGTH OF FLEXIBLE CULVERTS

Experience with underground flexible culverts has shown (8) that their flexural rigidity governs mainly the installation stages, while the compressive strength of the culvert material or joints governs the behavior under load as in a thin compression ring provided there is adequate backfill. The corresponding ring compression theory (Eq. 1) has been used successfully to design thin-walled plain and corrugated metal structures of different shapes, sizes and depths of backfill compacted to about 95 percent of the standard Proctor density. However, this approach does not take into account the actual properties of soils which may vary within wide limits, even at a specified Proctor density. Moreover, buckling may become important for larger structures than those built to date.

Therefore, in conjunction with the present model tests, a method has been developed to estimate the critical buckling stress of underground flexible culverts. As shown in the Appendix, the critical stress f_c of a circular culvert can be represented by

$$f_c = \frac{f_y}{1 + \dfrac{f_y (1 - m^2) A r^2}{C E I}} \qquad (3)$$

in which

A = effective cross-sectional area of culvert material;
C = buckling coefficient;
E = effective modulus of elasticity of culvert material;
f_y = effective yield stress of culvert material;
I = effective moment of inertia of culvert material;
m = Poisson's ratio of culvert material; and
r = radius of culvert.

For fills of which the deformation properties can be represented by a coefficient of soil reaction k, the theoretical buckling coefficients C_k have been derived in the Appendix. These coefficients are shown in Figure 5 in terms of the ratio r/L_k, where L_k is the relative stiffness of the culvert with respect to the soil and is

$$L_k = \sqrt[4]{\frac{E I}{(1 - m^2) k}} \qquad (4)$$

Further, it is shown for the important practical case of $r/L_k > 2$ that Eq. 3 can be simplified to

$$f_c = \frac{f_y}{1 + \dfrac{f_y A}{2} \sqrt{\dfrac{1 - m^2}{k E I}}} \qquad (5)$$

which is analogous to Eq. 2 and makes some allowance for accidental eccentricities and imperfections which can be expected in practice.

Frequently the deformation properties of fills are more closely represented by a modulus of deformation E_s and Poisson's ratio m_s. The corresponding theoretical buckling coefficients C_e have also been derived in the Appendix and are shown in Figure 5 in terms of the ratio r/L_e, where the relative stiffness

$$L_e = \sqrt[3]{\frac{2(1 - m_s^2) EI}{(1 - m^2) E_s}} \qquad (6)$$

Further, Eq. 3 yields for $r/L_e > 2$

$$f_c = \frac{f_y}{1 + f_y A \sqrt{\frac{(1 - m^2)(1 - m_s^2) r}{2 E_s E I}}} \qquad (7)$$

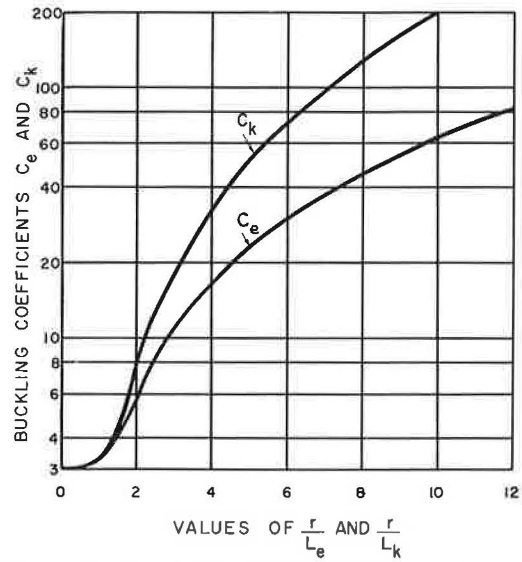

Figure 5. Theoretical buckling coefficients for circular culverts.

Eqs. 5 and 7 show that for good compaction of the backfill (when r/L_e and r/L_k exceed 2), the critical stress is practically independent of the radius of the culvert and the corresponding degree of compaction should increase with the radius. These equations have been plotted in Figure 6 for steel with E = 30,000,000 psi, f_y = 40,000 psi and m = 0.3, by using the parameters of $\sqrt{\frac{A}{kI}}$ (Eq. 5) and $A\sqrt{\frac{r}{E_s I}}$ (Eq. 7). Both parameters give practically the same result so an average curve can be used for fills represented by either a coefficient of soil reaction k or a modulus of deformation E_s.

These expressions were derived for circular culverts with a uniform soil resistance and would, therefore, apply mainly to cover heights exceeding the culvert diameter for instance. The results can, however, also approximately be used for other cases, such as flexible arches with a shallow cover, by taking the effective radius of the section and average values for the height and soil properties of the cover. In order to apply the

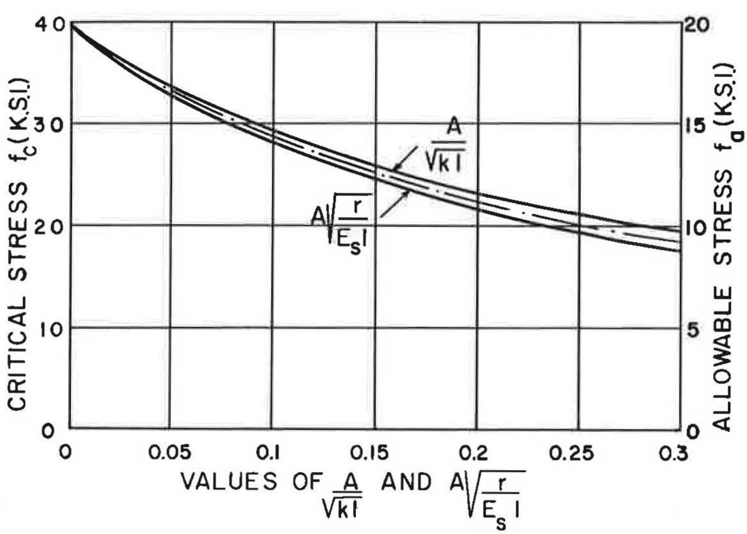

Figure 6. Theoretical critical and allowable stresses for steel culverts.

proposed analysis to an estimate of the critical stress governing the strength of flexible culverts in practice, the relevant physical properties of the culvert and fill have to be determined. Thus, the effective flexural rigidity EI of culverts should include the influence of flexibility of any joints, while the effective yield stress f_y should be based on the culvert material or joint strength, whichever is least.

Regarding the properties of the fill, conservative values of the coefficient of soil reaction k or of the modulus of deformation E_s should be chosen. The resistance of fills in the horizontal direction will usually govern in the case of sands and gravels. Thus, using an effective plate width of 1.5r causing buckling (see Appendix), the approximate effective coefficient of soil reaction (4) is as follows:

For clays

$$k = K_c/1.5r \tag{8}$$

For sands

$$k = K_s h/1.5r \tag{9}$$

in which

h = height of cover above culvert;
r = radius of culvert; and
K_c and K_s = constants of horizontal soil reaction for clays and sands, respectively.

Typical values of K_c and K_s (4) are given in Table 4. The values for sands apply to dry and moist materials and should be halved for submerged sands.

Moreover, the approximate modulus of deformation (4) is as follows:

For clays

$$E_s = K_c \tag{10}$$

For sands

$$E_s = K_s h \tag{11}$$

where the values of K_c and K_s are given in Table 4.

It is interesting to compare the values of the deformation properties of soils with the results of field observations on the deformation of flexible culverts under fills (7), summarized in Table 5. Using Eqs. 9 and 11 the analysis shows that the coefficient of soil reaction k and the modulus of deformation E_s of loose fill are roughly one-half that of compact material, and the corresponding deduced values of the constant of soil reaction K_s are also in good agreement with those given in Table 4. Moreover, for flexible culverts of average size (up to about 5-ft diameter) the coefficient of soil reaction k of the fill should not be less than about 20 pci, and greater values are suggested for larger structures. The corresponding modulus of deformation E_s of the fill should not be less than about 1,000 psi, and for culvert diameters exceeding about 5 ft, the value of E_s should increase roughly with the culvert diameter; about 200 psi per ft diameter.

These suggested values should be doubled for backfill near the structures, approximately, within a width of the culvert diameter which mainly affects their strength. The analysis of the field observations also shows that the ratio of r/L_k (or r/L_e) varies from about 1.5 to 3.5. A value less than 2 should not be used in practice to insure that the critical stresses are sensibly independent of the culvert diameter, as shown by Eqs. 5 and 7. In that case, the maximum radial deflection d is also practically independent of the flexural rigidity of the culvert and can be estimated from the approximate relationships based on Spangler's formula (3)

TABLE 4

VALUES OF CONSTANT OF SOIL REACTION FOR CLAYS AND SANDS

Clay		Sand	
Consistency	Constant K_c (psi)	Relative Density	Constant K_s (pci)
Stiff	500 - 1,000	Loose	1.5 - 4
Very stiff	1,000 - 2,000	Compact (medium)	4 - 12
Hard	Over 2,000	Dense	Over 12

TABLE 5

DEFORMATION PROPERTIES OF FILLS NEAR FLEXIBLE PIPE CULVERTS

Location	Item No.	Soil Type (C. = compact, L. = loose)	Cover Hgt., h (ft)	Culvert Diameter, 2r (ft)	Coef. of Soil Reaction, k (pci)	Modulus of Deformation, E_s (psi)	Constant of Soil Reaction, K_s (pci)	Radius ÷ Rel. Stiff., r/L_k
Ames, Iowa	1	L. loam	15	3.5	14	440	2.4	2.4
	2	L. gravel	16	3.5	32	1,020	5.3	2.9
	3	C. sand-clay	15	3.0	28	755	4.2	2.6
	4	L. sand-clay	15	3.0	13	350	1.9	2.2
	5	C. sand-clay	15	3.5	25	790	4.4	2.8
	6	L. sand-clay	15	3.5	15	470	2.6	2.4
	7	C. sand-clay	15	4.0	29	1,040	5.8	3.4
	8	L. sand-clay	15	4.0	14	505	2.8	2.8
	9	C. sand-clay	15	5.0	26	1,170	6.5	3.6
	10	L. sand-clay	15	5.0	12	540	3.0	3.0
Chapel Hill, N.C.	11	Sand	12	2.5	25	560	3.9	1.8
	12	Sand	12	2.6	56	1,320	9.2	2.3
	13	Sand	12	2.5	80	1,800	12.5	2.5
	14	Sand	12	1.7	35	525	3.7	1.3
	15	Sand	12	1.8	82	1,290	9.0	1.7
Culman, Ala.	16	C. crushed rock	137	7.0	190	12,000	7.3	3.2
McDowell, N.C.	17	C. sandy silt	170	5.5	40	1,980	1.4	1.7
Denver, Colo.	18	Crushed rock	41	15.0	10	1,350	2.7	2.9
Colorado	19	L. silty sand	13	10.0	4	360	2.3	1.7

$$d = 2.7\, p/k \tag{12}$$

or, substituting Eqs. 8 to 11,

$$d = 4\, pr/E_s \tag{13}$$

where p = average vertical soil pressure on culvert, and other symbols as before.

After the critical stress f_c of culverts has been estimated (Eq. 5 or 7), a safety factor of at least 2 should be used to determine the allowable axial stress f_a, as shown in Figure 6. The culvert can then readily be designed by the simple ring compression theory (Eq. 1), and the maximum deflection can be estimated (Eq. 12 or 13) to check that both the strength and deformation of the culvert are within permissible limits.

In the absence of published field data on the buckling of flexible culverts, the proposed analysis can be applied to a series of model loading tests by Watkins (6). In these tests plain steel culverts of about 2-in. diameter were embedded in a container filled with sand of various densities and they were loaded to failure by a vertical pressure applied to the ground surface. Using Spangler's formula of the deflection of flexible culverts (3), the coefficients of soil reaction k have been deduced from the experimental load-deflection curves, which were roughly linear until failure of the culverts. Substituting these values into Eq. 5, the theoretical soil pressures producing buckling failure of the culverts are found to be in good agreement with the observed values, if the yield stress is deduced from tests on culverts in very dense material when failure occurred by crushing of the material (Table 6).

Although further evidence, especially from full-scale observations of the ultimate strength of flexible culverts under various soil conditions is desirable, it may be concluded that the proposed method of analysis can be used to estimate the strength of culverts under fills in practice.

TABLE 6

RESULTS OF LOADING TESTS ON MODEL CULVERTS BY WATKINS (6)

Item No.	Coef. of Soil Reaction, k (pci)	Critical Soil Pressure[a] t = 0.04 in. Observed (psi)	t = 0.04 in. Theoret. (psi)	t = 0.01 in. Observed (psi)	t = 0.01 in. Theoret. (psi)
1	30,000	410	C[a]	175	C[a]
2	12,000	340	350	125	125
3	4,000	300	320	115	105
4	2,000	270	290	90	90
5	1,000	220	250	85	75

[a]t = culvert thickness; C = crushing failure.

CONCLUSIONS

1. A series of model tests on plain and corrugated steel culvert sheets bearing against dense sand, as well as some earlier tests on model culverts, shows that for small values of the coefficient of soil reaction or modulus of deformation of the backfill, and for small values of the flexural rigidity of the sheets, failure occurs by buckling. However, for large values of these parameters, failure occurs by yielding of the section.

2. The theory of elastic stability of plates has been extended to estimate the critical buckling stresses of circular sheets and culverts in an elastic medium, and simple equations and design charts are presented for use in practice.

3. To insure that the critical stresses in flexible culverts are sensibly independent of the culvert diameter, minimum values of the coefficient of soil reaction and modulus of deformation of fills have been suggested from an analysis of the deformation of culverts under fills in practice.

4. The results of the present model tests on circular sheets, and earlier experiments with model culverts, support the proposed method of analysis which can be used in conjunction with the ring compression theory to estimate the strength of flexible culverts under fills.

5. It is hoped that field observations will be made on the ultimate strength of culverts under various soil conditions for comparison with the proposed method of analysis.

ACKNOWLEDGMENT

The authors are indebted to the National Corrugated Metal Pipe Association for encouragement and support and many helpful discussions with C. L. Fisher and H. L. White of Armco Drainage and Metal Products, Inc. The junior author is also grateful for a Bursary of the National Research Council of Canada.

REFERENCES

1. Baikie, L. D., "Strength of Curved Plates Bearing Against Dense Sand." Unpublished M. E. thesis, Nova Scotia Technical College, Halifax, N. S. (1961).
2. Meyerhof, G. G., "An Investigation of the Bearing Capacity of Shallow Footings on Dry Sand." Proc. 2nd Int. Conf. Soil Mechanics, Vol. 1, p. 237 (1948).
3. Spangler, M. G., "The Structural Design of Flexible Pipe Culverts." Public Roads, Vol. 18, p. 217 (1938).
4. Terzaghi, K., "Evaluation of Coefficient of Subgrade Reaction." Geotechnique, Vol. 5, p. 297 (1955).
5. Timoshenko, S. P., and Gere, J. M., "Theory of Elastic Stability." McGraw-Hill, New York (1961).
6. Watkins, R. K., "Failure Conditions of Flexible Culverts Embedded in Soil." HRB Proc., 39:361-371 (1960).
7. Watkins, R. K., and Spangler, M. G., "Some Characteristics of the Modulus of Passive Resistance of Soil: A Study in Similitude." HRB Proc., 37: 576-583 (1958).
8. White, H. A., and Layer, J. P., "The Corrugated Metal Conduit as a Compression Ring." HRB Proc., 39:389-397 (1960).

Appendix

NOTATION

a = length of plate;
A = cross-sectional area of plate;
b = width of plate;
C, C_e, C_k = buckling coefficients of plate or culverts;
d = radial deflection of plate or culvert;
E = modulus of elasticity of plate or culvert;
E_s = modulus of deformation of soil;
f = unit stress in plate;
f_a = axial stress in plate or culvert;
f_b = buckling stress of plate or culvert;
f_c = critical stress in plate or culvert;
f_y = yield stress of plate or culvert;
h = height of cover above culvert;
I = moment of inertia per unit width of plate or unit length of culvert;
k = coefficient of soil reaction ("subgrade modulus");
K_c, K_s = constants of soil reaction;
L_e, L_k = relative stiffness of plate or culvert with respect to soil;
m = Poisson's ratio of plate;
m_s = Poisson's ratio of soil;
n = number of half-waves or order of buckling modes;
p = soil pressure on plate or culvert;
P_b = buckling force per unit width of plate or unit length of culvert;
r = radius of plate or culvert;
t = thickness of plate or culvert;
θ = center angle of half-wave.

BUCKLING OF CIRCULAR PLATES AND CULVERTS IN ELASTIC MEDIUM

If a long flat plate is supported by an elastic medium of which the reaction pressure at any point is directly proportional to the deflection and the plate is compressed by a uniformly distributed axial force acting along hinged edges, it can be shown (5) that the critical buckling force per unit width of the edge is

$$P_b = \frac{\pi^2 EI}{(1 - m^2)\, a^2}\left[n^2 + \frac{(1 - m^2)\, k a^4}{n^2 \pi^4 EI}\right] \qquad (14)$$

The value of n can be determined from the relationship

$$n^2 (n + 1)^2 = \frac{k a^4 (1 - m^2)}{\pi^4 EI} \qquad (15)$$

As k increases, the number of half-waves increases, and for a large number of waves, the critical buckling force is independent of the length of the plate and is

$$P_b = 2\sqrt{\frac{kEI}{1 - m^2}} \qquad (16)$$

A rigorous analysis of the buckling of cylindrical plates supported by an elastic medium is not yet available. However, an approximate solution can be obtained by combining the above results for flat plates with the analysis of the buckling of cylindrical plates under uniform external pressure for which the critical buckling force per unit width of the edge is (5)

$$P_b = \frac{EI}{(1 - m^2) r^2} \left(\frac{\pi^2}{\theta^2} - 1 \right) \tag{17}$$

or

$$P_b = \frac{\pi^2 EI}{(1 - m^2) a^2} \left(1 - \frac{\theta^2}{\pi^2} \right) \tag{18}$$

in which

a = arc length of half-wave, and other symbols are given in the notation.

Eq. 18 shows that for $\theta = 90^0$, which represents a quadrantal cylindrical plate and the lowest buckling mode of a circular culvert, the buckling force is three-quarters that of a freely supported flat plate (Eq. 14 for k = 0 and n = 1). As the angle θ decreases and the number of half-waves n increases, Eq. 18 rapidly approaches the corresponding value for a flat plate. Thus, for a circular culvert under an external pressure, Eq. 17 can be rewritten as

$$P_b = \frac{[(n+1)^2 - 1]\, EI}{(1 - m^2) r^2} \tag{19}$$

If the radial deflection curve of a half-wave of a cylindrical plate in an elastic medium compressed by a uniformly distributed axial force acting along hinged edges is assumed to be the same as that for a similar flat plate, the critical buckling force of a cylindrical plate will approach that of a flat plate as n increases. Thus, by substituting Eq. 19 into Eq. 14 the critical buckling force per unit length of a circular culvert in an elastic medium may be represented by

$$P_b = \frac{EI}{(1 - m^2) r^2} \left[(n+1)^2 - 1 + \frac{(1 - m^2) k r^4}{[(n+1)^2 - 1]\, EI} \right] \tag{20}$$

in which the term in large square brackets represents the buckling coefficient C. This coefficient, which is similar to that of a flat plate, can be evaluated in the same manner (see Eq. 15) and is shown in Figure 5 in terms of the ratio r/L_k, where

$$L_k = \sqrt[4]{\frac{EI}{(1 - m^2) k}} \tag{21}$$

For the fundamental buckling mode with n = 1, the buckling coefficient from Eqs. 20 and 21 is

$$C_k = 3 + \tfrac{1}{3}(r/L_k)^4 \tag{22}$$

which holds, approximately, for $r/L_k < 2$, while for higher buckling modes the buckling coefficient is nearly

$$C_k = 2\,(r/L_k)^2 \tag{23}$$

for $r/L_k > 2$.

Substituting Eq. 23 into Eq. 20 the critical buckling force for $r/L_k > 2$ is

$$P_b = 2\sqrt{\frac{k\,EI}{1 - m^2}} \tag{24}$$

and the corresponding buckling stress is

$$f_b = \frac{2}{A}\sqrt{\frac{k\,EI}{1 - m^2}} \tag{25}$$

as for flat plates and with the upper limit of the yield stress f_y of the plate.

Frequently the deformation properties of the elastic medium can be represented by a modulus of deformation E_s and Poisson's ratio m_s. In that case the above equations can be adapted by using the approximate relationship (4)

$$k = E_s/b \tag{26}$$

where b governs the deflection at the critical load. Thus, conservative estimates will be obtained by using b = a for flat plates and b = 1.5r for circular culverts when

$$k = E_s/1.5r \tag{27}$$

or

$$k = \frac{E_s}{2\,(1 - m_s^2)\,r} \tag{28}$$

because Poisson's ratio $m_s = 1/2$, approximately.

Substituting Eq. 28 into Eq. 20 the critical buckling force is

$$P_b = \frac{EI}{(1 - m^2)\,r^2}\left[(n+1)^2 - 1 + \frac{(1 - m^2)\,E_s r^3}{2\,[(n+1)^2 - 1]\,(1 - m_s^2)\,EI}\right] \tag{29}$$

where the term in large square brackets represents the corresponding buckling coefficient C_e. This coefficient has been so evaluated and is shown in Figure 5 in terms of the ratio r/L_e, where the relative stiffness

$$L_e = \sqrt[3]{\frac{2(1 - m_s^2)\,EI}{(1 - m^2)\,E_s}} \tag{30}$$

Further, proceeding as before,

$$C_e = 3 + 1/3\,(r/L_e)^3 \tag{31}$$

for $r/L_e < 2$, and approximately,

$$C_e = 2(r/L_e)^{3/2} \tag{32}$$

for $r/L_e > 2$ when the critical buckling force becomes

$$P_b = \sqrt{\frac{2\,E_s\,EI}{(1 - m^2)(1 - m_s^2)\,r}} \tag{33}$$

for $r/L_e > 2$.

In order to make some allowance for accidental eccentricities and imperfections of the culvert, the critical stress can conveniently be expressed by (5)

$$f_c = \frac{f_y}{1 + f_y/f_b} \tag{34}$$

Thus, substituting Eq. 20 into Eq. 34 the critical stress is

$$f_c = \frac{f_y}{1 + \dfrac{f_y(1 - m^2)Ar^2}{CEI}} \tag{35}$$

or, using Eqs. 25 and 33,

$$f_c = \frac{f_y}{1 + \dfrac{f_y A}{2}\sqrt{\dfrac{1 - m^2}{kEI}}} \tag{36}$$

for $r/L_k > 2$, and

$$f_c = \frac{f_y}{1 + f_y A\sqrt{\dfrac{(1 - m^2)(1 - m_s^2)r}{2E_s EI}}} \tag{37}$$

for $r/L_e > 2$.

Discussion

REYNOLD K. WATKINS, Professor and Head, Department of Mechanical Engineering, Utah State University—Dr. Meyerhof and Mr. Baikie have reported an important aspect of the structural performance of buried flexible conduits; namely, the interaction of ring crushing and hydrostatic buckling.

This discussion (a) encourages use of a column analogy for presentation of Meyerhof and Baikie's results; (b) provides a model study check for their concepts; (c) suggests a limit for conduit ring design if soil is poor and/or the installation is not well controlled; and (d) indicates areas for much needed additional study.

Model studies conducted at Utah State University are the prime source of the information and methods of presentation reported herein. Notation is as in Figure 7.

As a basis for design, ring failure is defined from observations on model tests (Fig. 8) to be either:

1. Deflection: (a) greater than some maximum permissible for adequate conduction and/or (b) causing excessive soil displacement; or
2. Buckling: (a) ring crushing (inelastic buckling); and/or (b) hydrostatic buckling (elastic buckling).

Deflection failure of the flexible conduit ring can be predicted by a method proposed by Spangler (9). Deflection $\Delta X/D$ for a given height of fill or vertical soil pressure p may be controlled partly by the conduit flexibility D^3/EI, and partly by the soil properties E' (soil type, moisture content, soil density, etc.).

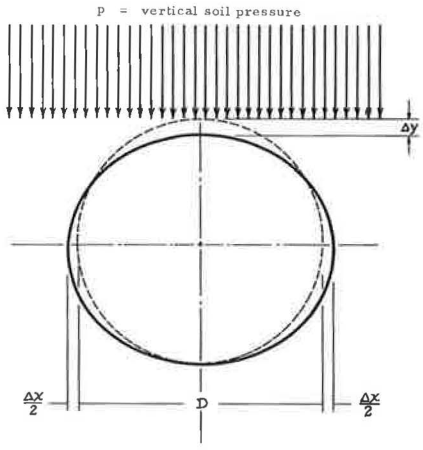

NOTATION

EI = ring wall stiffness per unit length of conduit, in kip-in.;
A = cross-sectional area of wall per unit length, in sq in.;
E' = soil modulus (corresponds to modulus of elasticity for elastic materials), in kips per sq in.;
D^3/EI = conduit ring flexibility, in sq in. per kip;
f_c = ring compression stress in conduit wall, in kips per sq in.;
f_y = yield stress, in kips per sq in.;
k = radius of gyration of wall cross-section, in in.; and
SF = safety factor.

Figure 7. Notation associated with the performance of buried flexible conduit.

Design by deflection will not be considered further in this discussion; however, it may not be disregarded. Model studies prove that failure can indeed occur by excessive deflection.

Figure 8 also shows a typical buckling failure as observed in model studies. White (8) has suggested that this type of failure is due to ring compression or crushing of the conduit wall (inelastic buckling). The design equation is

$$\frac{pD}{2A} = \frac{f_y}{SF} \tag{38}$$

Buckling failure has also been considered in terms of collapse due to a critical external hydrostatic pressure (elastic buckling). Brockenbrough (10) suggests the hydrostatic buckling equation

$$p\,\frac{D^3}{EI} = \frac{24}{SF} \tag{39}$$

as a conservative design limit except when ring compression controls. When does ring compression control, and when does hydrostatic buckling control? Is there an interaction of both effects calling for a further reduced design limit?

Interaction is suspected if one compares conduit strength with the strength of a column. A short heavy column having very low slenderness fails in crushing (Fig. 9). This is inelastic buckling. If the column is long and very slender, buckling failure will occur according to the Euler equation. This is elastic buckling. However, column tests show that there is an interaction range in which column strengths fall below both crushing and buckling.

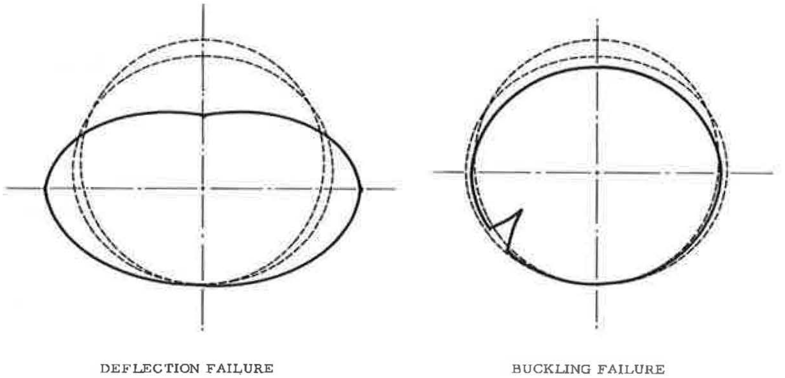

Figure 8. Two general types of structural ring failure of buried flexible conduits observed from model studies.

By analogous reasoning, ring buckling strength may be plotted for buried flexible conduits (Fig. 10). Therefore,

$$\frac{1}{E}\left(\frac{D}{k}\right)^2 = \frac{D^3}{EI}\left(\frac{A}{D}\right) \tag{40}$$

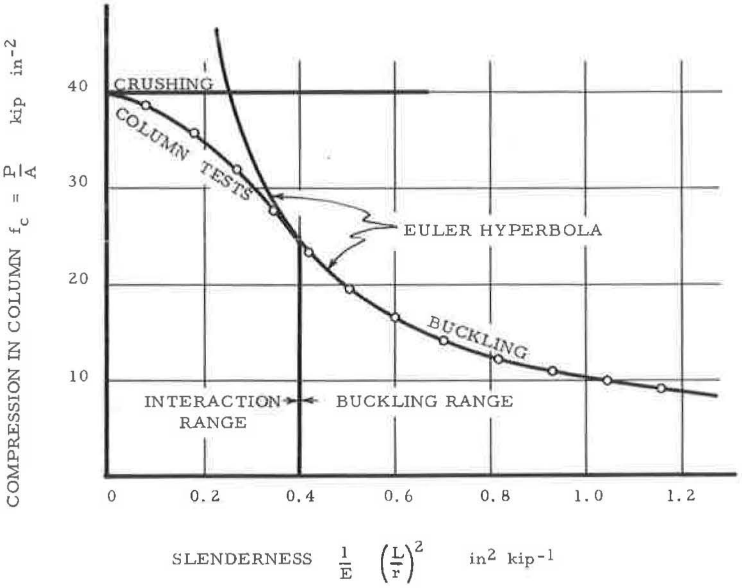

Figure 9. Typical presentation of column strength curves.

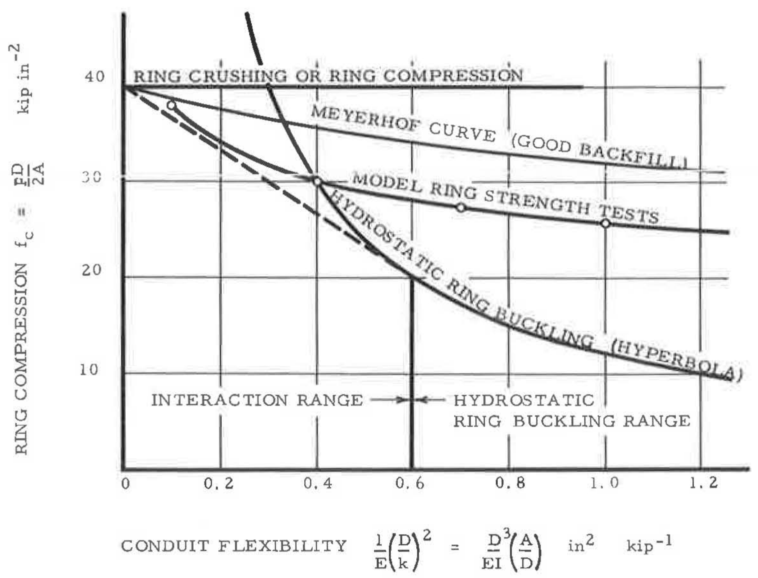

Figure 10. Ring buckling strength curves for buried flexible conduits.

TABLE 7

ALLOWABLE HEIGHT OF SOIL FILL IN FEET ABOVE TOP OF BURIED FLEXIBLE STEEL CONDUIT

Corrugation Configuration $\frac{1}{2} \times 2\frac{2}{3}$

Diam. (in.)	Gage 10	12	14	16	18	20	22	24	26	28	29
12	515	400	287	228	183	137	114	91	68	57	52
15	397	298	214	171	137	105	86	67	52	42	38
18	292	227	162	129	104	78	65	52	38	32	29
21	222	172	123	98	79	59	49	39	29	24	22
24	165	129	92	73	59	44	36	29	21	18	16
30	86	67	48	38	31	23	19	15	11	8	5
36	50	39	27	22	17	13	10	6			
42	32	25	18	14	10	5					
48	21	17	12	6							
54	14	10									
60	9										

Corrugation Configuration 1×3

Diam. (in.)	Gage 10	12	14	16	18	20	22	24	26	28	29
12	644	501	358	285	226	169	143	115	85	73	65
15	505	393	281	224	178	133	112	91	66	57	51
18	412	322	230	183	146	109	91	74	54	46	41
21	347	270	192	153	122	91	77	62	45	39	35
24	294	219	164	130	104	77	65	53	38	33	29
30	219	171	122	97	77	58	48	39	28	24	22
36	163	127	91	72	58	43	36	29	21	18	16
42	123	96	68	54	43	32	27	21	15	13	11
48	90	70	50	40	32	23	19	15	11	8	6
54	65	50	35	27	22	16	13	10			
60	47	36	25	21	16	11	9				
66	35	27	19	15	11	6					
72	27	20	14	11	7						
78	21	16	11	7							
84	16	12	7								
90	13	9									
96	10	6									

Design Assumptions:

1. Safety factor = 2. Allowable height of fill is approximately inversely proportional to the safety factor; e.g., the fill heights listed above must be reduced by half for a safety factor of 4.
2. Unit weight of soil is 100 pcf and H-20 liveload is on the surface.
3. Modulus of elasticity for the steel conduits is 33 kips per sq in.
4. Deflection must be checked.

where D^3/EI is the conduit ring flexibility on which the hydrostatic buckling formula is based.

The ring compression equation plots as a horizontal ring crushing line like the crushing line for a column. The hydrostatic buckling equation plots as a hyperbola like the Euler column formula for buckling. Like actual column tests, a series of model tests falls below both curves within an interaction range. This substantiates the authors' conclusion that ring compression and hydrostatic buckling interact. It is here suggested that diagrams like Figure 10 be used to present this interaction concept.

The model test curve of Figure 10 rises above the hydrostatic buckling curve as conduit flexibility increases. This is because the soil was not hydrostatic. Actually the soil developed some strength and partially supported the ring. Conduit strength curves for highly plastic soil (hydrostatic) approach the hydrostatic buckling curve. Plots for dense, angular, non-plastic soil approach the ring compression line. The quality of the soil around the conduit determines where the conduit strength curve falls between these two extremes. If the backfill is good and conduit flexibility is low (i.e., if the conduit shape is not altered during loading) the ring compression theory may be an adequate basis for design. However, for questionable backfill and/or high conduit flexibility, the hydrostatic buckling theory is safer. Additional experimental work is needed to determine where the strength curve will fall between these two extremes, depending on soil properties.

Until such work is done, it is recommended that for average installations, conduit strength be conservatively defined as shown by the dashed line in the interaction range and the hydrostatic hyperbola in the hydrostatic ring buckling range.

In these model tests the observed yield point is 40 kips per sq in. In actual installations the yield point may be different depending on the material. For example, a conservative yield point for corrugated culvert steel is 33 kips per sq in. The equation for design strength in the interaction range is then

$$\frac{pD}{2A} = \left[33\text{ksi} - \frac{363}{16} \; \frac{D^3}{EI} \left(\frac{A}{D}\right) \right] \div \text{SF} \tag{41}$$

for values of D^3/EI (A/D) less than 0.72 sq in. per kip.

Above this value the design strength is given by Eq. 39. For those who prefer design tables, this could be recorded in a form of Table 7. If such tables are not published, it would be convenient to publish the values D^3/EI and D/A for use in design equations. Table 7 is based on a safety factor of 2. Using such conservative design limits there is no apparent need for a greater safety factor for average installations. The height of fill is based on an assumed unit weight of soil of 100 pcf with an H-20 live load. Information on conduit deflection should accompany any published design data.

Table 7 includes some height of fill values for a proposed deeper corrugation referred to as a 1 × 3 corrugation. The deeper corrugation has better resistance to buckling.

It is recommended that the effect of soil properties on conduit buckling be investigated. Conduit deflection at buckling failure should be investigated for various soil-conduit systems. The adequacy of the vertical soil pressure p as used in the design formulas should be checked.

REFERENCES

9. Spangler, M. G., "Soil Engineering." Internat. Textbook Co., Scranton, Pa., p. 433 (1960).
10. Brockenbrough, R. L., "A Theoretical Evaluation of Two Corrugation Profiles for Corrugated Metal Pipe Culverts." Memorandum, U. S. Steel Corp., ARL Proj. 90.12-017 (Feb. 1962).

G. G. MEYERHOF and L. D. BAIKIE, Closure—The authors are grateful to Professor Watkins for his interesting contribution to the discussion and they agree that the column analogy would provide a good basis for the presentation of their test results on the strength of steel culvert sheets. This is shown by a comparison of the observed maximum axial stress with the theoretical critical stress of the sheets at failure given in Table 3, although the range of relative stiffnesses of the sheets to the soil or the "conduit flexibility" was rather limited. A wider range of conduit flexibilities was studied by Professor Watkins in his series of model tests, which also support the authors' analysis, as shown in Table 6.

The model test curve (Fig. 10) compares well with the theoretical interaction relationship between ring crushing and buckling, as expressed by Eq. 3 if the buckling coefficient C is taken to be about 15. This value is 5 times the hydrostatic buckling coefficient of 3 and represents a high degree of compaction of the sand in the model tests. Even for average installations when the ratio of culvert radius to relative stiffness (r/L) is about 2, the theoretical buckling coefficient would be about 2 to 3 times the hydrostatic value (Fig. 5). The corresponding design curves in Figure 6 can then be used to estimate the strength of steel culverts in terms of their stiffness (or "flexibility") as well as the deformation (or "strength") properties of the soil. On the other hand, the authors believe that Eq. 41 and Table 7 proposed on the basis of hydrostatic ring buckling would give unduly conservative estimates in practice.